University of California, Merced

Evaluating the Transcriptome of the Settled Polyp of the Robust Coral, *Montastraea faveolata* when Infected with the Competent Symbiont, by Microarray Analysis

A thesis submitted in partial satisfaction of the requirements for the degree

Master's of Science

in

Quantitative and Systems Biology

by

Aubrie Elise O'Rourke

Committee in charge:

Doctor Monica Medina, Chair

Doctor Michael Cleary

Doctor Nestor Oviedo

2011

DEDICATION

First and foremost this body of work is dedicated to my Father, Peter O'Rourke, for always encouraging me to follow my dreams and to never give up. To my Mother, Kathryn O'Rourke, for always encouraging my creativity. To my Grandfather, William Grupen, for being the figure that peeked my interest in science. To my Grandmother, Doris Grupen, for always seeing the world from a logical and loving point of view. To my family for their undying support and genetics.

I am very thankful.

EPIGRAPH

Man has not yet caught up with the Genius of Nature.

William Grupen

It is not birth, marriage, or death, but gastrulation, which is truly the most important time in your life.

Lewis Wolpert

TABLE OF CONTENTS

Signature Page……iii

Dedication……iv

Epigraph……v

Table of Contents……vi

List of Figures……..vii

List of Tables……viii

Acknowledgments……ix

Abstract……..x

Introduction……1

Materials and Methods……6

Results……11

Discussion…….....23

References……34

List of Figures

Figure 1: Heat map of Mf1.05b treatment's differentially expressed genes…11

Figure 2: Heat map of EL1 treatment's differentially expressed genes……12

Figure 3: Heat map of differentially expressed genes common to Mf1.05b and El1 treatments……13

Figure 4: Gene distance matrix for all treatments……13

Figure 5: qPCR results bar graph…….....14

List of Tables

Table 1: Fold change for Mf1.05b differentially expressed genes……15

Table 2: Fold change for EL1 differentially expressed genes……17

Table 3: Fold change for differentially expressed genes common to Mf1.05b and EL1 treatments……20

ACKNOWLEDGEMENTS

I would like to thank my advisor, Professor Monica Medina, for giving me the opportunity to study the wonderful subject of coral biology.

I would like to thank the Medina lab group, both past the present, for the wealth of knowledge that they bestowed upon me. These amazing people include: Zer Vue, Shinichi Sunagawa, Michael deSalvo, Erika Almeyda Diaz, Collin Closek, Bishoy Hanna, Emmanuel Buschiazzo, and Kristen Marhaver.

I would like to thank Professor Christian Voolstra, for his microarray knowledge and scientific guidance.

I would like to thank UCMerced for coming to my hometown and bringing hope for the brighter futures of its youth.

ABSTRACT OF THE THESIS

Evaluating the Transcriptome of the Settled Polyp of the Robust Coral, *Montastraea faveolata* when Infected with the Competent Symbiont, by Microarray Analysis

by

Aubrie Elise O'Rourke

Master of Natural Science in Quantitative and Systems Biology

University of Californa, Merced, 2011

Professor Monica Medina, Chair

The robust clade coral, *Montastraea faveolata* engages in a symbiosis with the microeukaryote, *Symbiodinium.* We used this experiment in combination with results from previous microarray experimentation in coral of the same species to provide a time series that begins before metamorphosis and ends after the transition from planula to polyp in *Montastraea faveolata*. This time series allows us to evaluate the effects of symbiosis upon the host transcriptome at various stages of metamorphosis and days after infection. The experiment in this study takes sixteen day old polyps, infected them at 7days with the competent and incompetent symbiont strains and collected them 9 days later. A

microarray analysis was preformed in order to target genes that are involved in the calcification process of settled calcifying polyps. A baseline for the genes to be expected in a settled polyp was provided by the gene list found in current literature that discussed the transcriptomic changes seen in uninfected settling polyps of *Acropora millepora*. Our experimentation revealed genes novel that were not found in that study and this suggests that the differential expression of these genes is a direct result of the symbiosis and not as a reaction to settlement. In this experiment we found an up-regulation in developmental genes and genes involved in vesicular trafficking among other genes that are common to the settlement process. We also see that unlike the earlier infection time points, settled calcifying polyps are exhibiting significant alternations in the transcriptome as a result of infection with the competent symbiont.

Introduction

The coral-algal symbiosis is fundamental to the functioning of a healthy reef. In healthy corals, the metabolic output of the symbiotic organisms interacts and confers to the host the ability to grow, reproduce and resist disease. The readily observable bleaching events around the globe serve as the impetus for conducting research in order to better understand the breakdown of the coral reef ecosystem. Fortunately, molecular experimentation has provided new ways for the coral biologist to understand the complexity of this ecosystem and to better understand symbiosis.

Symbioses are common throughout the plant, fungi, and animal kingdoms. A classical example in the plant kingdom includes the symbiotic fungus, Mycorrihizae, which lives on the roots of plants. These fungi fix limiting nutrients that are critical for plant metabolism and in return gain access to carbohydrates from the plant's metabolism (Smith, 1997). Another example are lichen, these are fungus that engage in a symbiosis with either an alga or cyanobacteria. In this example, the host maintains a moist environment in which the symbiont can live and the photosymbiont generates sugars to be used by the host's metabolism (Bates, 2011).

Some classically studied animal symbiosis include the parasitic wasp *Asobara tabida* and its bacterial partner *Wolbachia*, the Hawaiian bobtail squid *Euprymna scolopes* and its symbiotic bacterium *Vibrio fischeri.* The human body also engages in various symbiosis with microorganisms, a prime example being

the biota found in the gut that are necessary for healthy digestion. Furthermore, the subject of this study, the cnidarian-*Symbiodinium* association is one of the few mutualistic eukaryotic symbioses and one of the most breathtaking as a successful symbiosis between the two can create large colorful reef structures that support an ecosystem for many other species.

V. fischeri demonstrate a developmental influence on *E. scolopes* as it actually constructs the light organ in which it will reside, the newly hatched squid collects bacteria from the seawater, the bacteria then induce apoptosis in the tissue, which then becomes the light organ (Nyholm & McFall-Ngai, 2004). In the case of *A. tabida,* normal female development is dependent on *Wolbachia.* When the females are treated with antibiotics that kill the symbiotic bacteria, the wasps are unable to produce mature oocytes, and thus cannot reproduce (Dadeine et al*.,* 2001). In the case of the cnidarian, *Montastraea faveolata* and its photosymbiont, *Symbiondinium,* the host provides a home for the symbiont while the symbiont provides sugars to feed the host's metabolism. There is evidence from previous experimentation to suggest that such a symbiosis also enhances calcification rates, immunity, and vesicular trafficking within the host.

Previous investigations

Experiments have been performed in order to better understand the effect of symbiosis on the developing polyp in both *Fungia scutaria* and *Monstastraea faveolata*. In *F. scutaria,* 6 day old larvae were sampled 48 hours post infection and very few measurable transcriptional changes were observed during the

onset of the coral-dinoflagellate endosymbiosis (Schnitzler and Weis, 2010). The authors suggest that the choice of sampling time might have missed the window of transient differential expression. However, it is observed again from another study on *M. faveolata* where two treatments with different symbionts were used to evaluate the onset of symbiosis, that 30 minutes after infection, the transcriptomic response did not deviate from that of the control. In the samples taken 6 days after infection the host transcriptome again remained unaltered by the competent symbiont (one known to successfully infect the host). However, in the treatment where an incompetent symbiont (transient infection that does not persist inside the host's tissues) was the infectious agent, the transcriptome was significantly altered (Voolstra, 2009).

In order to see the effect of the competent symbiont upon the calcifying polyp, we conducted a symbiont infection experiment with settled sixteen-day-old polyps of *M. faveolata*. Polyps were exposed to one of two symbiont strains, one known to establish a successful symbiosis with this host (i.e., a "competent symbiont") and one known to fail in establishing symbiosis in this host (i.e., an "incompetent symbiont"). The calcified polyps were collected 9 days after infection and host transcriptomes were examined and compared using microarray technology.

The results from our findings in combination with the previous studies show a time course which includes planula larvae and unattached metamorphosed polyps exposed to the competent symbiont and collected 30 minutes and 6 days after exposure, in addition to the newly generated time point

of settled calcifying polyps exposed to the competent symbiont and collected nine days later. The 30-minute time point showed little if any transcriptomic change in either treatment. The six day time point revealed that the host transcriptome remains unaltered by the presence of the competent symbiosis, suggesting that the competent symbiont goes somewhat unnoticed, while the incompetent symbiont elliicts large transcriptomic differential expression in genes affecting cell adhesion/ cytoskeleton, cell cycle/growth/differentiation, protein biosynthesis, protein degradation, response to stress, metabolism, regulation of transcription, immune response, and RNA modification.

The hypothesis for our current experimentation is that at nine days post infection we will begin to see the changes in the transcriptome that will suggest how the competent symbiont is contributing to the calcification process. The acquisition of the correct algal symbiont is important for coral health because skeleton deposition is thought to be greatly enhanced by the competent symbiosis. This concept is referred to as 'light-enhanced calcification' (Kawaguti and Sakumoto, 1948). We expect to see a differential expression of genes involved in the calcification process.

Recent experimentation in the complex coral *Acropora millepora*, used microarray technology to evaluate the transcriptomes of eight day old planula at the time points of 30 minutes and 4 hours post exposure to larval settlement cues (Grasso, 2011). The results from this experiment provide a baseline and allow us to see what genes are differentially expressed in the case of uninfected settling larvae. The results of this experimentation find that coral planula appear to

anticipate metamorphosis and suggest that the larvae are “primed” for settlement and enable the speed at which metamorphosis occurs. The genes that show significant differential expression in this settlement induction experiment include genes concerning calcium handling, apoptosis, immunity, stress response, calcium metabolism, formation of the skeletal organic matrix, calcium-sequestering proteins (calreticulin), protein folding (heat shock proteins), cell adhesion (lectins).

In our investigation we expect to see these same types of genes among other differentially expressed genes. In our experimental design we have introduced the competent and incompetent symbiont to settled calcifying polyps. These polyps may still exhibit vestigial signs of their recent metamorphosis in the transcriptome. The above mentioned settlement paper give us an idea of what we should expect to see, it will be the genes that are not common to the settlement gene list that will give us an idea as to what genes are differentially expressed as a direct result of the infection by the competent symbiont.

Materials and Methods

Collection and Experimental Setup

Egg-sperm bundles were collected from adult colonies of *Montastraea faveolata* on 10 September 2009 in Puerto Morelos, Quintana Roo Mexico. From the La Bocana cite (20° 52'28.77"N and 86°51'4.53"W) at 4 meters depth. Fine mesh nets (1.75 m wide, 2 m high) were placed over 6 colonies before spawning and secured to surrounding rocks by small weights without causing harm to the colony. Buoyant gamete bundles were collected in plastic jars fixed to the top of each cone-shaped net. Gametes from distant colonies were mixed 15 minutes after spawning and the fertilized embryos were raised to the swimming planula stage in the lab. The embryos were kept in zoox-free water that was sterilized with an ultraviolet lamp. Initially the embryos were raised in a large plastic cooler (150 liters) with no water flow and a 50% water change was done daily. For the experiment, the embryos were allowed to further develop in 1 liter polypropylene containers filled with zoox-free water and this water was changed 50% every 2 days. Seven days after spawning, planulae that were assigned randomly into three separate 1 liter treatments (n = 3 replicates per treatment, 75 planulae per replicate) were infected with either a competent zooxanthellae symbiont (MF1.05b; see below for details about symbiont strains), an incompetent symbiont (CassEL1), or no symbiont (control). The final concentration of zooxanthellae in each treatment was 1000 cells ml^{-1}. Nine days after infection (16 days after spawning), settled, infected polyps were collected, preserved in

RNAlater (Ambion), and stored at -80°C. Infection was confirmed using a microscope; 5 polyps were taken every 2 days and flattened under a cover slip on a microscope slide to check for the presence of zooxanthellae.

Symbiont strains (*Symbiodinium* sp.) were chosen based on their rejection or acceptance by *M. faveolata* in previous infection experiments. The strain Cass EL1, (from *Symbiodinium* Clade A3) was isolated from the zooxanthellate jellyfish *Cassiopeia* sp., from Kaneohe Bay, Hawaii by RNA Kinzie III. The strain Mf1.05b (from *Symbiodinium* Clade B1) was isolated from *M. faveolata* in the Florida Keys by M. A. Coffroth. Cultures of these zooxanthellae were maintained in Puerto Morelos at 24°C under 12 hours of light (fluorescent lights with 50 umol quanta m^{-2} s^{-1}) and 12 hours of darkness in F/2 medium containing antibiotics.

Isolation of total RNA from settled polyps

Settled coral polyps were collected from the experimental containers using sterile cotton swabs, which were placed in preservative along with the polyps. To isolate total RNA from the swabs, the tubes with RNAlater and cotton swab were centrifuged for 10 min at 12,000 x rcf. Swabs were wiped across the interior surfaces of the tubes using tweezers to collect any pelleted coral tissue from the tubes. The swab was then placed in a mortar containing liquid nitrogen and ground into a powder. The powder was removed with a spatula and placed in a 2.0 ml screw cap tube. To each tube, 1.5 ml of Qiazol (Qiagen) was added. Samples were then homogenized for 2 min using a Mini Bead-Beater (Biospec) with both 0.1 mm and 0.55 mm silica beads. To each tube, 0.45 ml of chloroform

was added; tubes were then vortexed for 30 seconds and incubated at RT for 3 min. Each sample was centrifuged at 12,000 x rcf for 15 min at 4°C. From the aqueous layer, 500 μl was transferred to a new tube and RNA was precipitated by adding 500 μl of 100% isopropanol and 5 μl (20 ng/μl) of glycerol. To pellet the RNA, tubes were vortexed for 30 s, then incubated at RT for 10 min, then centrifuged for 15 min under the same conditions as above. The isopropanol was removed and RNA pellets were twice washed with 70% EtOH and centrifuged at maximum speed for 5 min at 4°C. The wash and centrifugation step was repeated a second time. RNA pellets were then air-dried for 10 min and resuspended in 50 ul RNase-free water. The RNA was further purified using the RNeasy Mini Kit (Qiagen). The RNA quantity and quality were assessed using a NanoDrop ND-1000 spectrophotometer.

Probe preparation and hybridization to microarrays

For each experimental replicate, 1 ug of total RNA was amplified using the MessageAmp II aRNA kit (Ambion) according to manufacturer's instructions. Because some of the replicates did not have enough starting material, this procedure was repeated for all replicates a second time.

For each experimental replicate, 3 μg of aRNA were primed with 3 μl of random pentadecamers for 10 min at 70°C. A reverse transcription was carried out with the primed replicates for 2 h at 50°C using a master mix (Invitrogen) containing a 4:1 ratio of aminoallyl-dUTP to TTP (Ambion). After reverse transcription, the single-stranded RNA was hydrolyzed by incubating the reverse

transcription with 10 μl 0.5M EDTA and10 μl 1M NaOH for 15 minutes at 65°C. Following hydrolysis, the reactions were cleaned using the MiniElute Cleanup kit (QIAGEN). Cy3 and Cy5 dyes (GE Healthcare) were dissolved in 18 microliters dimethyl sulphoxide (DMSO), these dyes were assigned to their respective tubes and allowed to couple to the aminoallyl-dUTP groups that were previously incorporated into the cDNA. This coupling was carried out in the dark for two hours. The dye-coupled cDNA was cleaned using the MiniElute Cleanup kit (QIAGEN). The appropriate Cy3-labeled sample was combined with the appropriate Cy5-labeled sample then added to a hybridization buffer containing 025% SDS, 25 mM HEPES, and 3x SSC. The samples were then heated to 99°C for 2 minutes then pipetted into the space between the post-processed microarray and an mSeries Lifterslip (Erie Scientific). The post processing of the microarray involved ultraviolet crosslinking at 60mJ, a washing with a 'shampoo' treatment (3x SSC, 0.2% SDS at 65°C), followed by a blocking step with 5.5 g of succinic anhydride dissolved in 335 ml 1-methyl-2-pyrrilidinon and 15 ml of sodium borate, and then dried by centrifugation.

The samples consisted of three treatments with three biological replicates each. Each treatment was tagged with the Cy3 dye (green fluorescence). Three microliters from each of the treatment's amplified RNA was combined to create a pooled reference sample. Each treatment was hybridized to the array with a pooled reference sample that was labeled with the Cy5 dye (red fluorescence).

The microarray consisted of 10,930 PCR-amplified cDNAs spotted in duplicate on poly-lysine-coated slides yielding a microarray with 21,860 total features.

Data Analysis

All hybridized microarrays were scanned into GenePixPro and saved as TIFF files. A manually constructed annotation grid file was overlaid and fit for feature extraction. All nine scanned images were converted to .mev files using TIGR Express Converter. Files with annotation overlay were then loaded into MIDAS version 2.19 (TIGR) for normalization of spot intensities. Output from MIDAS was then opened in Excel and the log intensity ratio for each gene on each of the nine hybridizations was calculated. Only genes that hybridized for 2 out of 3 experimental replicates of each treatment were further analyzed. SwissProt and GO annotations were included in the log2 ratio file, The file was opened with Multiple Experiment Viewer version 4.2 (MeV). A SAM analysis was carried out under a 5% false discovery rate (FDR) in order to determine differential gene expression. The lists of significant differentially expressed genes were generated by their statistical comparison to the uninfected control samples (Figures 1,2,3). Microarray results were confirmed by qPCR. The cDNA triplicate samples were run on a ninety-six well plate with CCHW7292 as the housekeeping gene and run against the genes SCRiP 2,4,8, Peroxidasin (AOSF997) and CAON 1465. The qPCR results reflect the microarray results for the tested Mf1.05b samples.

RESULTS

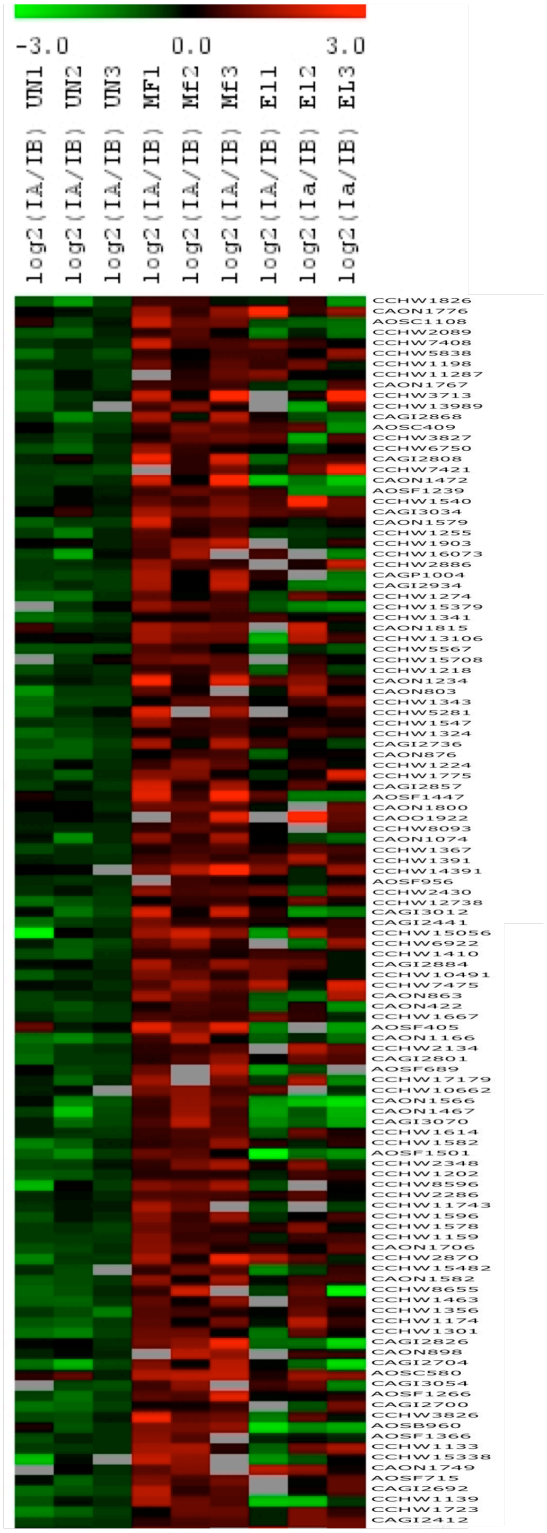

Figure 1: (left,below) Heat map of the differentially expressed genes at a 5% false discovery rate for the competent Mf1.05b treatment. Red represents an up-regulation and green a down-regulation. EL samples are more similar to the control expression for all genes.

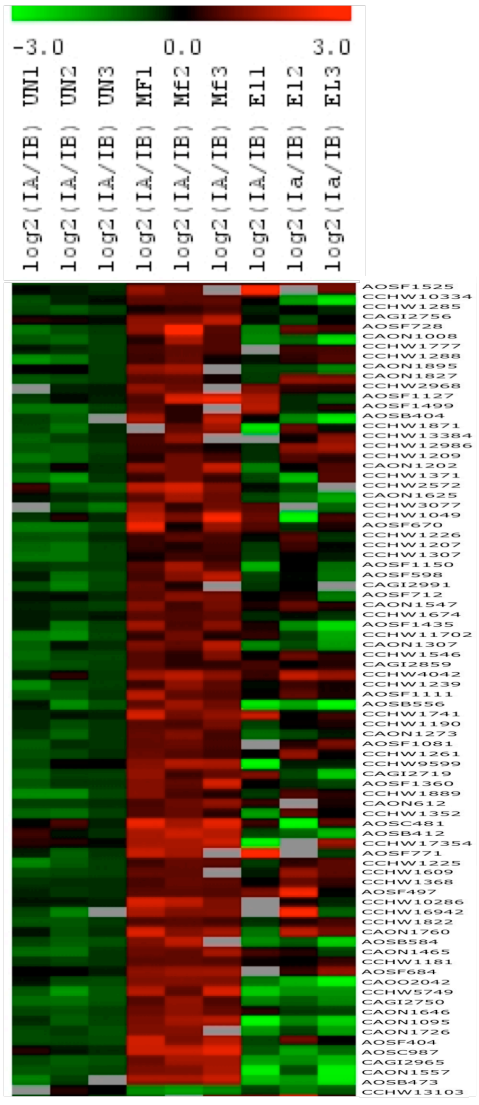

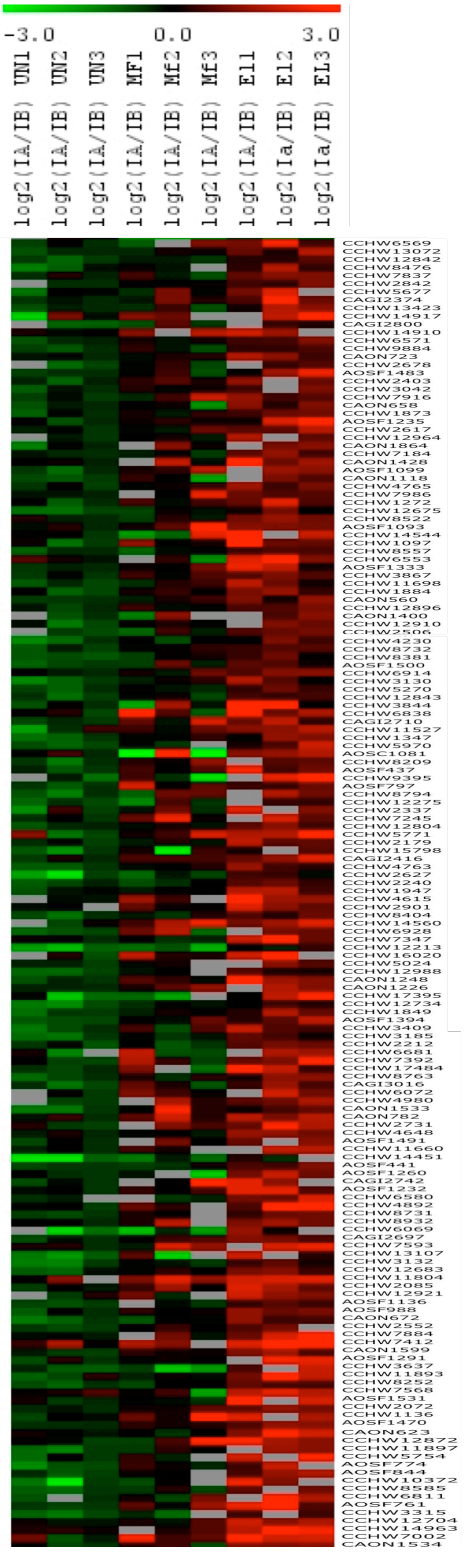

Figure 2: (left,below) Heat map of the differentially expressed genes at a 5% false discovery rate for the competent EL1 treatment. Red represents an up-regulation and green a down-regulation. Mf1.05b samples are more similar to the control expression for all genes.

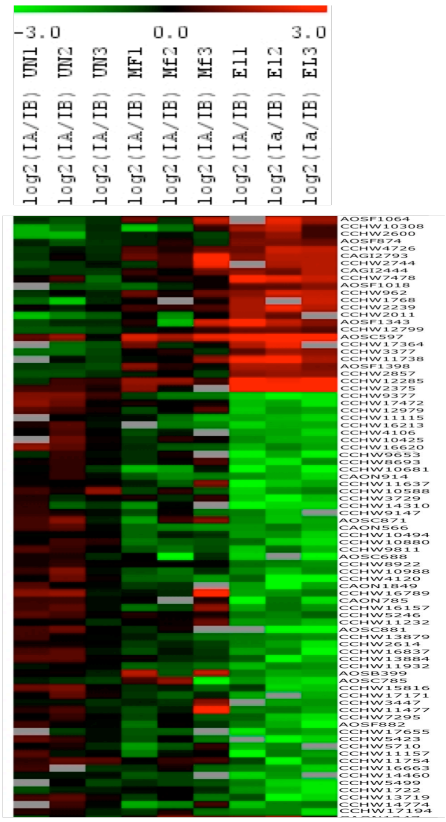

Figure 3: (below) Heat map of the differently expressed genes at a 5% false discovery rate that are commn to the two treatments, Mf1.05b and EL1.

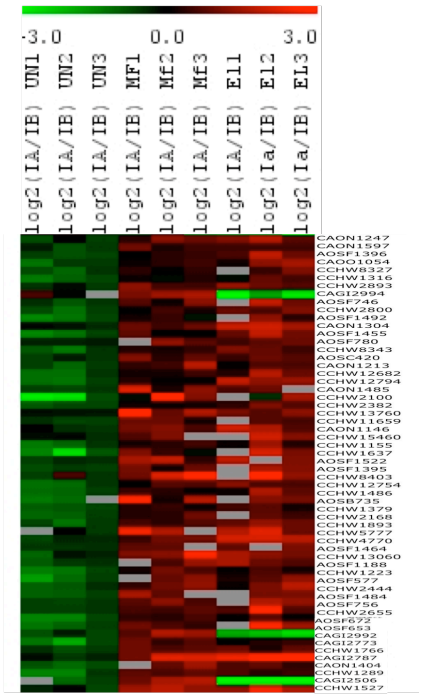

Figure 4: (Below) Gene Distance Matrix illustrating how the 3 replicates of the separate conditions (control, Mf1.05b, EL1 treatments) are more similar in differential expression pattern to themselves rather than to samples of the other conditions.

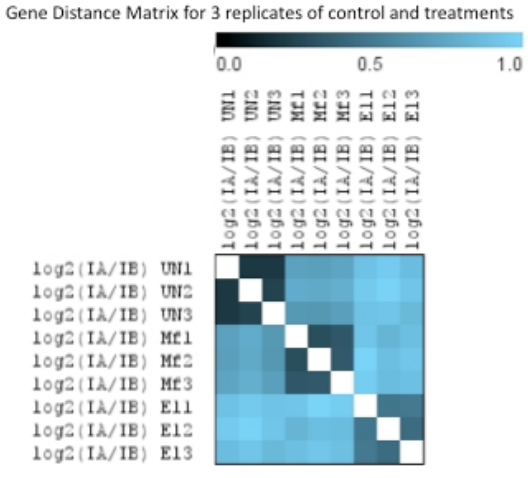

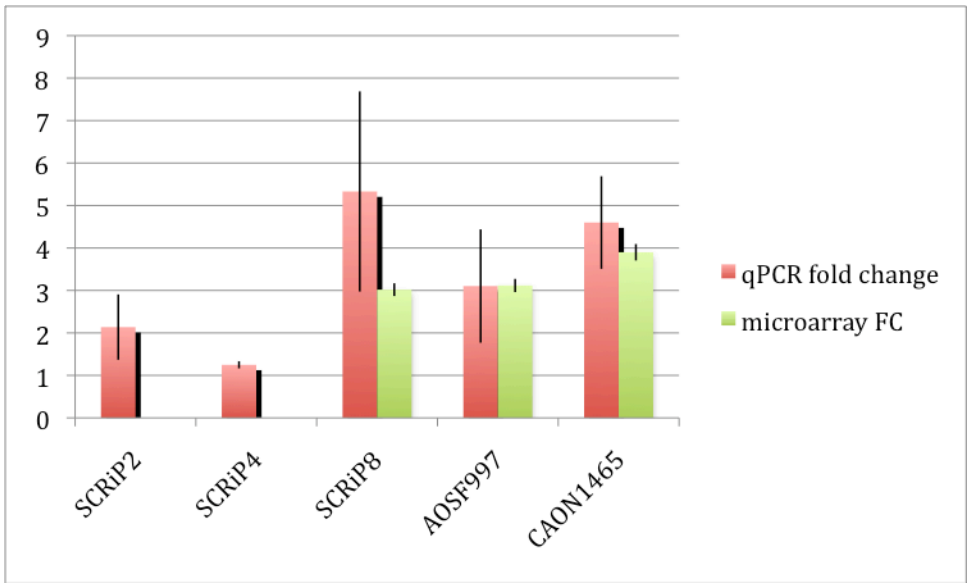

Figure 5: qPCR results confirming the fold-changes found by the microarray results for the tested Mf1.05b triplicate samples. SCRiP 2 and 4 were not found by the microarray but confirmed to be present by qPCR at a less significant fold change. The red bars signify the fold change found with quantitative PCR. The green bars signify the fold change found by the microarray analysis for Mf 1.0b samples.

Table 1: Significant differentially expressed genes (5% false discovery rate) for the Mf1.05b samples. First column: Gene ID, second column: Gene Annotation, third column: Fold Change. Genes in blue are discussed in body of the paper.

"Mf1.05b 5%":		
CCHW13103	Carbohydrate sulfotransferase 4-celladhesion	0.31057918
CCHW1391	Acyltransferase 3	1.8440185
CCHW2286	Scavenger receptor type C	1.8714616
CCHW8093	NADH dehydrogenase subunit 5	1.882976
AOSF956	-	1.8953066
CAON1767	-	1.8973747
CCHW1667	-	1.8994812
AOSF1239	-	1.9213351
CAON1800	-	1.931092
CCHW1367	Tetratricopeptide repeat protein 9C	1.9445227
CCHW1614	Predicted protein	1.9726242
CCHW1540	ER lumen protein retaining receptor 2	1.9849483
CCHW1410	Extracellular peptidase inhibitor (Fragment)	1.9905063
CCHW1674	-	1.9985843
CCHW1218	Superoxide dismutase [Mn]	2.0073085
CAGI2412	Putative uncharacterized protein (Fragment)	2.0193243
CCHW15708	-	2.0265195
CCHW1202	-	2.0290272
CAON422	Neutral alpha-glucosidase AB	2.0302653
CCHW1341	Predicted protein	2.0456305
CCHW1324	Guanine nucleotide-binding protein G(q) subunit alpha	2.0741465
CCHW5838	Transcription elongation factor 1 homolog	2.0824742
CCHW1198	-	2.096807
AOSC409	Predicted protein	2.1000102
CCHW2089	Cytochrome c oxidase III	2.1047735
CCHW11287	C-Myc-binding protein	2.105604
CCHW5567	-	2.1078217
CCHW2134	-	2.111467
CCHW1777	FAD dependent oxidoreductase	2.117185
CCHW13106	Predicted protein	2.118125
CCHW12738	ECM protein	2.1228476
CCHW3827	lysyl-tRNA synthetase	2.135207
CCHW1285	Predicted protein (Fragment)	2.1579297
CAON876	-	2.1590574
CCHW1578	-	2.1666806
CCHW7421	-	2.1862328
CAGI3034	-	2.2006986
CCHW15379	-	2.213448
CCHW10334	Uncharacterized N-acetyltransferase yjgM	2.21361
AOSF497	-	2.2176774
CCHW12986	-	2.2268353
CAGI2700	-	2.244818
CCHW1224	-	2.2776802
CCHW1547	-	2.279539
CCHW1368	Quinone oxidoreductase-like protein 1	2.283377
CCHW2430	-	2.2894132
CCHW15482	-	2.3047345
CAGI2859	Putative uncharacterized protein	2.3144279
CAON1815	Ras-related protein Rab-10	2.3223882
CCHW1255	Mitochondrial import inner membrane translocase subunit Tim8	2.323925
CCHW10662	-	2.329269
CCHW2886	collagen-peptidase inhibitor activity	2.3305013
CCHW1226	-	2.3314962
CCHW7475	-	2.358384
CCHW1159	UV excision repair protein RAD23 homolog B	2.364342
CAON1776	-	2.366552
AOSF712	-	2.3695352
AOSF1525	cell adhesion	2.372397
CCHW1343	-	2.3838272
CCHW2968	-	2.389037
CCHW1181	Protein jagged-1b	2.3956838
CCHW1274	-	2.3999808
CCHW13989	Chromosome undetermined scaffold_186, whole genome shotgun sequence	2.4138982
CAGI2441	CCAAT/enhancer-binding protein gamma	2.4148536
CCHW1207	Uncharacterized protein C14orf45 homolog	2.4155412
CCHW1826	Signal recognition particle 54 kDa protein	2.416818
CAON1827	-	2.4325569
CCHW1356	-	2.439385
CCHW10491	Predicted protein	2.4429774
CAON1749	cytochrome b	2.4459467
CCHW1261	-	2.4633045
CAGI2756	-	2.4726
CCHW1190	Uncharacterized protein C14orf133 homolog	2.4908943
CCHW1307	Histidine triad nucleotide-binding protein 1	2.4933684
AOSF1366	-	2.4946573
CCHW1609	Predicted protein	2.5112782
CAON803	-	2.520113
AOSF1081	-	2.5289664
CAGI3054	neurobeachin	2.5579512
CAON1895	-	2.5685267
CCHW1822	-	2.5727806
CCHW11743	-	2.5844069
CAON1547	-	2.5906813
AOSF1499	-	2.5990713
AOSF715	-	2.5996542
CCHW1903	E3 ubiquitin-protein ligase LRSAM1	2.6082976
CAGI2884	reverse transcriptase-like protein	2.608721
CAON863	Na+-transporting ATP synthase	2.6119564
AOSC580	-	2.6130092
CAON1706	Predicted protein	2.6195676
CCHW1174	Protein salvador homolog 1	2.6269817
AOSB960	-	2.6307476
AOSC1108	Thioredoxin reductase 1, cytoplasmic	2.636598
CCHW6922	-	2.6492188
CCHW6750	Cell division control protein 42 homolog	2.6493068
CCHW1775	Putative uncharacterized protein	2.6542401
CAON1625	-	2.6616168

Table 1 (continued): Significant differentially expressed genes (5% false discovery rate) for the Mf1.05b samples. First column: Gene ID, second column: Gene Annotation, third column: Fold Change. Genes in blue are discussed in body of the paper.

CAGI2801	Ankyrin repeat and SOCS box-containing 8	2.7079873
AOSF684	-	2.7192752
CCHW1596	;Predicted protein	2.7360625
CAGI2991	Pol-like protein	2.7437015
CCHW1209	Forkhead box protein O1	2.7704997
CCHW1139	-	2.7917163
CCHW17354	-	2.7965496
CCHW17179	Acetyl-CoA acetyltransferase, mitochondrial	2.8028398
CCHW1546	NADH dehydrogenase subunit 5	2.8040466
CAON612	Activating transcription factor 4-like protein	2.8078108
CAON1273	-	2.8097475
AOSF1501	-	2.814048
CCHW1352	-	2.8366547
CCHW13384	Protein AATF	2.8429291
CCHW2348	Chymotrypsinogen B	2.8434117
CCHW1288	Thioredoxin, mitochondrial	2.8865993
AOSF689	Pol-like protein	2.8964527
CCHW1723	Transcription factor HES-1	2.8996146
CCHW1463	Inositol hexakisphosphate kinase 1	2.924075
CAON898	hypothetical protein	2.927742
AOSF1150	-	2.9371407
CAON1566	-	2.944475
CCHW7408	-	2.9789655
CCHW1582	-	2.9795823
CCHW4042	Scleractinian cysteine-rich protein	3.0191205
CAOO2042	-	3.0233407
CCHW16073	TNF receptor-associated factor 5	3.0527112
CCHW9599	Protein BTG1	3.053611
CCHW1225	Novel protein similar to H.sapiens CEP78, centrosomal protein 78kDa (CEP7	3.0548422
CCHW1301	-	3.0731285
CAGI2719	-	3.093361
CCHW1371	Nuclear distribution protein nudE-like 1	3.0935094
CCHW11702	Peroxidasin	3.1175277
CAON1074	-	3.135431
CCHW1871	Gamma-soluble NSF attachment protein	3.1447349
CAON1646	Nucleoside diphosphate kinase B	3.1965501
CAGI3070	-	3.2126257
CAON1202	-	3.2252505
CAON1726	-	3.2291236
CCHW1133	-	3.234488
AOSB412	DNA polymerase epsilon catalytic subunit A	3.2650058
AOSF405	-	3.2722163
CAON1008	-	3.2753835
CAON1307	-	3.2815278
CCHW3077	Chromosome undetermined scaffold_5, whole genome shotgun sequence	3.282053
CCHW1239	Predicted protein	3.2924962
AOSF1435	-	3.339294
CAON1582	Solute carrier organic anion transporter family member 4A1	3.3512833
CAOO1922	Serologically defined colon cancer antigen 1 homolog	3.432471
CAGP1004	-	3.4674513
CCHW8596	Gamma-interferon-inducible lysosomal thiol reductase	3.4837484
CCHW1741	Calbindin-32	3.4912786
AOSB556	-	3.5067823
CAON1467	-	3.516052
CAGI2934	-	3.5217566
CAGI2692	-	3.5661182
AOSF1111	s:P38062;Methionine aminopeptidase 2	3.5701377
CAGI2857	C-type lectin 3	3.5873947
CCHW1889	Arylsulfatase B	3.6394658
CAGI2826	-	3.6506615
CAGI2750	-	3.6734169
CAON1579	-	3.6775076
AOSF598	-	3.6781535
CAGI2736	-	3.7595031
CCHW8655	Protein FAM96A	3.809697
AOSC481	-	3.8190854
CAON1465	-	3.900043
CCHW16942	Predicted protein	3.9064753
CCHW10286	-	3.9182804
CCHW5281	-	3.9215477
AOSB404	-	3.9438841
CAGI2868	Kringle-containing transmembrane protein 1	3.9553483
CAON1166	-	3.983984
CCHW2572	Tubulin alpha chain	3.984999
CAON1557	-	3.9896934
AOSF1360	-	4.0353484
AOSF771	-	4.0534
CAGI2808	-	4.090101
CCHW15338	-	4.114008
CCHW1049	Serine hydrolase-like protein	4.1221104
AOSB584	-	4.1502566
CAON1095	-	4.160373
CAGI2965	-	4.2352414
CAON1760	-	4.2671194
CCHW3826	-	4.291883
AOSF1266	-	4.328091
AOSC987	-	4.4248643
AOSF1447	Glutathione S-transferase Mu 5	4.4447865
CCHW15056	-	4.6012907
CAGI3012	-	4.619504
CAGI2704	-	4.6600003
AOSF1127	-	4.765525
CAON1234	Coiled-coil domain-containing protein 94	4.9577374
AOSF404	-	5.0186777
CCHW2870	Ci-Notch protein	5.2033014
AOSB473	-	5.636429
CCHW3713	-	5.8009033
AOSF670	-	6.121565
CCHW5749	Ankyrin repeat and IBR domain-containing protein 1	6.3070364
CAON1472	-	6.4872465
CCHW14391	-	6.9810786
AOSF728	-	

Table 2: Significant differentially expressed genes (5% false discovery rate) for EL1 samples. First column: Gene ID, Second column: Gene Annotation, Third column: Fold Change. Genes in purple are down-regulated, genes in blue are up-regulated and both are discussed in paper.

"EL1 5%":		fold change
CCHW9377	Guanine nucleotide-binding protein subunit beta-like prot	0.08683771
CCHW17472	-	0.13256805
CCHW10681	-	0.15784653
AOSC881	40S ribosomal protein S12	0.16861913
CCHW14310	Putative phospholipase B-like 1	0.18135256
CCHW3729	-	0.18245687
CCHW11637	-	0.1848004
CCHW16620	-	0.18519194
CCHW10588	-	0.1890434
CAON785	-	0.19014724
CCHW4120	Tubulin alpha-1D chain	0.19064377
CCHW13719	-	0.1922926
CCHW9653	40S ribosomal protein S11	0.19273956
CCHW16789	-	0.1927641
AOSC871	-	0.19483322
CAON1849	-	0.19922838
CCHW12979	Predicted protein	0.1998247
CCHW16213	-	0.2015894
CCHW16837	14-3-3-like protein GF14-D	0.20213126
CCHW13884	60S ribosomal protein L10	0.20474057
CCHW8693	40S ribosomal protein S11	0.2172964
CCHW10425	-	0.22235729
CCHW15816	Ubiquitin	0.22372457
AOSF882	CCAAT/enhancer-binding protein gamma	0.22571151
CCHW4106	60S ribosomal protein L18a	0.22869
AOSC688	Chymotrypsinogen A	0.22925216
CCHW10988	Adenosylhomocysteinase B	0.23147924
CCHW10880	-	0.23247804
CCHW5423	-	0.23521355
CCHW11157	10 kDa heat shock protein, mitochondrial	0.24553691
CCHW9811	60S ribosomal protein L13	0.24805455
CAON914	60S ribosomal protein L7a	0.25200912
CCHW11754	Phosphoglycerate kinase	0.2524327
CCHW11115	-	0.25722688
CCHW9147	-	0.26265836
CAON566	40S ribosomal protein S10	0.26672572
CCHW16157	Arginine and glutamate-rich protein 1	0.2784661
CCHW7295	-	0.28148124
CCHW2614	Peptidyl-prolyl cis-trans isomerase	0.28252113
CCHW17171	60S ribosomal protein L13	0.28650308
CCHW16663	60S acidic ribosomal protein P0	0.2893303
CCHW10494	Oligosaccharyltransferase complex subunit OSTC	0.3021119
CCHW5499	-	0.303341
CCHW17194	-	0.30628628
CCHW17655	Protein FAM81A	0.31382567
AOSC785	Cytochrome c	0.31932223
CCHW11477	-	0.3196732
CCHW5246	-	0.32777485
CCHW11232	-	0.33033356
CCHW1722	Soma ferritin	0.33169478
CCHW14774	Endoplasmic reticulum-Golgi intermediate compartment p	0.33392495
CCHW13879	Prothrombin	0.34565446
AOSB399	Predicted protein (Fragment)	0.34691495
CCHW11932	60S acidic ribosomal protein P1	0.34717494
CCHW8922	DnaJ homolog subfamily C member 13	0.35007414
CCHW14460	Coiled-coil-helix-coiled-coil-helix domain-containing prote	0.35167542
CCHW5710	-	0.35667124
CCHW3447	Mitochondrial import receptor subunit TOM40 homolog	0.40751562
CCHW7986	Acyl-CoA dehydrogenase family member 11	1.9759141
CCHW9884	Glyoxalase/bleomycin resistance protein/dioxygenase	2.0604026
CAGI2800	-	2.125608
CCHW8557	Guanine nucleotide-binding protein G(o) subunit alpha	2.1837883
CCHW12842	15-hydroxyprostaglandin dehydrogenase [NAD+]	2.1848547
AOSF1093	-	2.1914449
CCHW2678	Prefoldin subunit 1	2.218089
CCHW2842	Phosphatidylethanolamine-binding protein 4	2.2226386
CCHW3867	cAMP-dependent protein kinase type II-alpha regulatory s	2.2236154
CCHW7837	Uncharacterized oxidoreductase SERP2049	2.226188
CCHW12275	Predicted protein	2.2354977
CCHW12896	-	2.235734
CCHW8732	-	2.2428682
CCHW12843	Glutathione S-transferase 1	2.2697258
AOSF797	-	2.3039706
AOSF1136	-	2.3132935
CCHW8522	Pre-mRNA-splicing factor syf2	2.3153505
CCHW6914	Mediator of RNA polymerase II transcription subunit 26	2.3251805
CCHW2506	-	2.329268
CCHW6571	Predicted protein	2.3297863
CCHW3042	Probable methyltransferase C20orf7, mitochondrial	2.3393018
CCHW7184	-	2.3492472
AOSF1500	-	2.3506634
CCHW5270	Putative uncharacterized protein	2.3536332
CCHW1873	Transmembrane emp24 domain-containing protein	2.3601732
CCHW5024	-	2.3969796
CCHW2240	-	2.4197161
CCHW12988	Thiosulfate sulfurtransferase/rhodanese-like domain-cont	2.4379628
CCHW7916	Hemagglutinin/amebocyte aggregation factor	2.4453413
CCHW2552	-	2.4642086
CCHW8209	Placenta-specific gene 8 protein	2.4664562
CCHW8381	Histone deacetylase complex subunit SAP30L	2.4724693
AOSF441	-	2.4777863
CCHW2212	Coiled-coil domain-containing protein 6	2.479298
AOSC1081	Tyrosine-protein kinase Fgr	2.480673
CCHW4648	-	2.4993463
CAON1118	-	2.5010793
CCHW8932	-	2.5067263

Table 2 (continued) : Significant differentially expressed genes (5% false discovery rate) for EL1 samples. First column: Gene ID, Second column: Gene Annotation, Third column: Fold Change.

AOSF1491	-	2.5261385
CCHW12804	Uncharacterized protein yxiE	2.5307922
CCHW2403	Elongation factor 1-alpha	2.5509048
CCHW8252	Caltractin (Fragment)	2.5517144
CCHW4765	CUB and sushi domain-containing protein 2	2.560298
CCHW12964	Uncharacterized protein YML079W	2.5630608
CAON658	Myosin-2 heavy chain	2.564625
CCHW8404	Spliceosome RNA helicase Bat1	2.574739
CAGI2697	-	2.5784762
CAON1400	-	2.5853634
CCHW12734	-	2.615477
CCHW12851	-	2.618405
CCHW2072	Band 4.1-like protein 3	2.624753
CCHW2617	-	2.6416857
CCHW3185	-	2.6553438
CAON1864	Dynein gamma chain, flagellar outer arm	2.6693814
CCHW12675	Tissue alpha-L-fucosidase	2.6725593
CCHW15798	-	2.674059
CCHW12910	-	2.6798608
CAON723	-	2.6823545
CCHW14910	-	2.689531
CAON560	-	2.7143629
CCHW1884	-	2.7408173
CCHW3315	Eukaryotic translation initiation factor 4E type 2	2.7571857
CAON1534	-	2.7652183
CAON1533	-	2.7682388
AOSF1470	-	2.7934659
CCHW6928	Predicted protein	2.7941816
AOSF988	Predicted protein	2.806695
CCHW4980	Prefoldin subunit 5	2.8224516
CCHW3132	-	2.8254364
AOSF874	-	2.8359268
CAON1226	LWamide neuropeptides	2.8414364
CCHW4230	Lipopolysaccharide-induced tumor necrosis factor-alpha	2.850386
CAON782	-	2.859978
CCHW13072	-	2.8821855
CCHW8585	-	2.8907933
CCHW12213	La-related protein 6	2.8929057
CCHW7568	-	2.9129283
CCHW4763	-	2.9207337
CAON1599	-	2.9224188
CCHW12683	-	2.9468362
CCHW2179	Lipopolysaccharide-induced tumor necrosis factor-alpha	2.9650605
CCHW12799	-	2.9743845
CAGI3016	Putative uncharacterized protein	2.9843373
CCHW13423	Putative uncharacterized protein	3.0284088
CCHW6072	-	3.0544088
AOSF1018	-	3.0592527
AOSF1099	-	3.0726357
AOSF1260	-	3.1160688
CCHW8763	X-ray radiation resistance-associated protein 1	3.1252801
CAGI2710	-	3.1359148
CAON672	-	3.1366296
CCHW8476	Cell division control protein 42 homolog	3.1496325
CCHW12704	CCR4-NOT transcription complex subunit 3	3.1790676
CCHW11527	General transcription factor 3C polypeptide 1	3.1857295
CCHW11804	Predicted protein (Fragment)	3.188606
CCHW14560	-	3.1916013
CCHW7245	Predicted protein	3.2184556
CCHW11660	-	3.2225306
CCHW12921	-	3.227071
CCHW6681	-	3.2579176
CCHW11698	Homeobox protein OTX2-B	3.259668
CCHW1947	Histone H2B.3	3.2613022
CCHW2627	-	3.2677863
CCHW1347	-	3.2853968
CCHW2901	-	3.2868514
CCHW5677	-	3.2967887
CCHW1849	Egg protein	3.3448935
CAGI2793	Putative uncharacterized protein	3.355468
CAGI2416	-	3.3738682
CCHW6580	Transcription initiation factor TFIID subunit 13	3.4103928
CCHW14451	-	3.425153
CAGI2444	Dynein gamma chain, flagellar outer arm	3.4726415
CCHW1272	-	3.5091934
CCHW8794	-	3.512373
AOSF1394	-	3.5382419
CCHW3130	Lipase member I	3.5599985
AOSF844	-	3.5837955
CCHW2085	-	3.5946946
CCHW2337	Mediator of RNA polymerase II transcription subunit 28	3.6021798
CCHW7593	Putative uncharacterized protein (Fragment)	3.6164443
CAOO943	Putative uncharacterized protein	3.6202803
CCHW3409	Lipopolysaccharide-binding protein	3.6692085
CCHW2744	-	3.6759448
CCHW1136	-	3.7263436
CCHW5970	Diphthamide biosynthesis protein 1	3.7315328
CCHW2857	Pancreas transcription factor 1 subunit alpha	3.7704568
CCHW6569	-	3.7938566
CCHW3637	-	3.810177
CCHW11897	-	3.8187418
CCHW5771	-	3.8255534
CAGI2742	Predicted protein	3.851002
CCHW6838	Endoplasmic reticulum lectin 1	3.8962038
CCHW4726	-	3.9744039
CCHW14917	-	3.9865055
CAGI2374	Putative serine/threonine-protein kinase C05D10.2	4.0195785
CCHW2239	Guanine nucleotide-binding protein-like 3 homolog	4.020951

Table 2 (continued) : Significant differentially expressed genes (5% false discovery rate) for EL1 samples. First column: Gene ID, Second column: Gene Annotation, Third column: Fold Change.

CCHW962	Pogo transposable element with KRAB domain	4.0331736
AOSF1398	-	4.0471134
CCHW2731	Cytochrome c oxidase copper chaperone	4.0861483
CCHW12872	-	4.154194
CCHW3377	Hemagglutinin/amebocyte aggregation factor	4.1867223
CAON623	-	4.1903915
AOSF1483	-	4.1957393
AOSF1232	-	4.219291
CCHW7002	Predicted protein	4.2894287
CCHW6069	-	4.306455
AOSF1333	-	4.307539
AOSF437	-	4.3098726
AOSF774	-	4.3279
CCHW7392	D-amino-acid oxidase	4.3868775
CCHW2600	Elongation factor 2	4.531584
AOSF1064	-	4.6017
CCHW16020	Predicted protein	4.6391025
CAON1428	Vesicle-associated membrane protein 3	4.710008
AOSF1291	Homeobox protein SIX1	4.7197285
CCHW7347	-	4.7319984
CCHW13107	Putative all-trans-retinol 13,14-reductase	4.785649
AOSF1235	-	4.8982053
CCHW7412	Neurexin-4	4.9195986
CCHW2011	-	5.045757
AOSF1531	-	5.0982757
CCHW7884	28S ribosomal protein S2, mitochondrial	5.1692834
CCHW10308	Hepatocyte growth factor receptor	5.2620597
CCHW6811	Uricase	5.2637625
CCHW5754	Calumenin	5.2653384
AOSC597	-	5.38939
CCHW1097	-	5.41639
CCHW9395	Death-associated protein 1	5.676782
CCHW11893	-	5.7178106
CCHW1768	-	5.763329
CCHW7478	Predicted protein	5.8707647
CCHW4615	-	5.9151807
CCHW17364	;Predicted protein	5.951003
CCHW17395	-	6.504358
CCHW12285	-	6.521428
AOSF1343	Predicted protein	6.526136
CCHW11738	-	6.5728216
CCHW2375	UPF0732 protein v1g81173	6.670851
CCHW10372	Programmed cell death protein 5	6.7215586
CCHW14963	Urea active transporter, isoform A	6.785455
CCHW6553	NADH dehydrogenase [ubiquinone] flavoprotein 2	7.184449
AOSF761	Proapoptotic caspase adapter protein	7.537747
CCHW14544	Tachylectin-2	7.7746215
CCHW17484	-	7.822047
CCHW4892	-	8.0049715
CCHW3844	-	9.552357
CAON1248	-	19.628765

Table 3: Significant differentially expressed genes (5% false discovery rate) common to both the Mf1.05b and EL1 treatments. First column: Gene ID, Second column, Gene annotation, Third column: Mf fold change, Fourth column, EL fold change.

Common		MF fold change	EL fold change
CCHW2382	ATP-binding cassette sub-family E member 1	1.8489949	2.756409
AOSF1396	-	1.8755479	3.599253
CCHW8327	-	1.9694028	2.6358747
CAON1304	Enkurin	1.9969517	4.098027
CCHW1316	Tripartite motif-containing protein 2	2.0344024	2.6196437
CAOO1054	-	2.0627291	3.4404533
CCHW1379	-	2.0749083	2.4169626
CCHW2800	-	2.106998	3.1784277
CCHW15460	-	2.1494908	3.4700184
CCHW12794	UPF0451 protein C17orf61 homolog	2.1521416	5.5311956
CCHW8343	Predicted protein	2.1534529	3.0888557
CAON1597	Bromodomain-containing protein 8	2.1574042	2.0241237
AOSF1464	-	2.2095356	2.4297411
CCHW2655	Prefoldin subunit 6	2.2204309	4.62944
CCHW12682	Serologically defined colon cancer antigen 1	2.2259302	3.8401103
CCHW1486	-	2.2293186	3.5402403
AOSF780	Myosin-2 essential light chain	2.242705	2.0104516
CCHW2893	-	2.261414	2.61884
AOSF1492	-	2.29082	3.1516364
CAON1146	-	2.310691	3.4899237
CCHW1155	-	2.3491993	2.961032
CAON1247	-	2.3759882	3.0916443
AOSC420	-	2.384333	2.1669436
CCHW4770	N-acetyllactosaminide beta-1,3-N-acetylglucosaminyltransfera	2.415783	5.316365
CCHW11659	-	2.4218123	2.1040545
CCHW1893	Sacsin	2.4499142	3.3986669
CAGI2994	-	2.4674785	0.17259482
AOSF746	-	2.5234146	3.3033187
CCHW1766	-	2.5259533	2.3291788
AOSF1395	Phospholipase A2, membrane associated	2.549617	3.2426183
AOSF1455	-	2.5597484	4.9294477
CCHW12754	-	2.5944273	3.2712054
CCHW2168	liposaccharide binding protein	2.6175718	2.5348117
AOSF756	-	2.7339869	3.5763986
AOSF672	-	2.8585973	2.6707842
AOSF1188	-	2.8796036	3.237433
AOSF653	-	2.9736423	6.496589
CCHW1223	-	3.0729892	2.4850755
CCHW2444	-	3.1340368	3.559386
CAON1213	-	3.2753386	2.243045
CCHW1289	-	3.3551989	2.8033319
AOSF1484	S-adenosylmethionine synthetase	3.4482355	3.1195977
CCHW1527	-	3.4912076	4.4266906
CAON1404	Alanine aminotransferase 2-like	3.5423105	2.787993
CAGI2992	-	3.5525377	0.32926002
AOSF1522	-	3.5714884	3.3337128
CAGI2773	Fibropellin-1	3.6073656	2.6666863
AOSF577	-	3.653196	3.5782025
CCHW5777	-	3.7137923	3.3820982
CCHW1637	Plasma glutamate carboxypeptidase	3.8927178	6.829254
CAON1485	Predicted protein	4.0527177	2.2951481
CAGI2506	Putative uncharacterized protein	4.1129274	0.12166159
CAGI2787	Putative uncharacterized protein	4.604186	9.682424
CCHW8403	Platelet-activating factor acetylhydrolase IB subunit beta	4.6633883	12.314907
CCHW13060	Abhydrolase domain-containing protein 4	4.8526626	3.3189056
CCHW13760	Leucine-rich repeat-containing protein 47	5.227213	2.3017552
AOSB735	-	6.5751414	3.043914
CCHW2100	Putative methyltransferase NSUN7	35.707073	4.8167667

Using a five percent false discovery rate, 257 genes were found to be up-regulated and one gene down-regulated in coral polyps infected with the competent symbiont Mf1.05b (Figure 1, Table 1). 244 genes were up-regulated and 61 genes were down-regulated in the coral polyps infected with the incompetent symbiont EL1 (Figure 2, Table 2). Of the 562 total genes to show

significant differential expression between the treatments, 59 genes were common to both treatments, three of the genes were down-regulated in the EL1 treated polyps while up-regulated in the MF1.05b treatment, and the remaining were up-regulated (Figure 3, Table 3).

In order to illustrate the codevelopment of the competent symbiont and the host, a microarray experiment was performed where settled calcifying polyps were collected 9 days after infection. Two treatments were performed, one in which coral polyps were exposed to a competent symbiont and another where polyps were exposed to the incompetent symbiont. Genes that showed significant differential expression through microarray analysis are: (1) symbiont uptake and maintenance genes, including Rab10, Arylsulfatase B, and a protein containing the BEACH domain, (2) classical developmental genes such as Notch and its ligand Jagged, as well as FOXO1, (3) immune response genes, and (4) calcium sequestration genes as indicated by the numerous transcripts containing EF-hand calcium binding domains sequence that is characteristic of genes in the extracellular matrix.

These results suggest that the mechanisms used during the onset of symbiosis for the coral host *M. faveolata* with its microeukaryote *Symbiodinium* may be similar to the processes used when a bacterial symbiosis or parasitism is established. It appears that at 9 days after infection, the competent symbiont in *Montastraea faveolata* has established itself in the host tissue within a symbiosome. It is most likely maintained in the coral polyp by the device of the

Rab10 gene, and the algae's numbers are maintained by an up-regulation of this gene.

In addition, Notch signaling is up-regulated which facilitates healthy development and cell to cell communication. It appears that the germ line is developing, energy out-put is enhanced as mitochondrial genes are up-regulated and calcium sequestration is high, immune response genes are in effect, and apoptosis pathways are regulating healthy management of the symbiont uptake and maintenance. Meanwhile, the incompetent symbiont is causing the host to up-regulate apoptosis genes and down-regulate ribosomal proteins necessary for translation of amino acids, while causing an up-regulation in innate immunity and protein quality control genes.

Discussion

Competent Infection

Microarray analysis of settled sixteen-day-old calcifying polyps that were exposed to competent symbionts nine days prior to sampling allowed for a glimpse into the dynamic process of codevelopment that occurs between the *Montastraea faveolata* polyp and the algae *Symbiodinium.* In order for codevelopment to begin, the symbiont must successfully infect the host tissue. This may begin by intracellular contact and recognition that is modulated by surface macromolecules as occurs in most biological systems where two cells interact (Frazier & Glaser 1979). Evidence to support this in the phylum Cnidaria, includes studies conducted on the *Hydra-Chlorella* model where the algal surface macromolecules are signaling to the endodermal cells of *Hydra* (Muscatine & Pool 1979) for the uptake of the algae *Chlorella.* On the other hand, it has been proposed that the initial phagocytotic events during establishment of the coral-algal symbiosis is non-specific and that the selection of the correct symbiont occurs after phagocytosis. The microarray study described here provides support for the first hypotheses in that a C-type lectin is up-regulated in the analysis, and weaker support for the second hypothesis as evidenced by the involvement Ras-related Rab 10 gene's differential expression.

In the first case, the C-type lectin requires the binding of a calcium ion in one domain and a second bound calcium ion in a second domain in order for glycan from the symbiont or bacteria to initiate intercellular contact. (E. M. Wood-Charlson and V. M. Weis 2009). It is because C-type lectins are conserved

components in the innate immune response that their presence alone cannot lead to the determination of whether the initial phagocytotic event is specific or non-specific. Being that the specificity qualification is not met, we are led to the consideration for the second hypothesis, where competent symbiont recognition occurs after phagocytosis.

Possible qualification of the second scenerio comes from the differential expression of the Ras-related Rab 10 within the transcriptomes of the sampled polyps. This suggests that the polyp maybe using a post-phagocytotic mechanism that has been previously characterized in the gram-positive bacteria, *Mycobacterium tuberculosis* as it infects the gastrointestinal cells of its host. *Mycobacterium* is phagocytosed by its host cell and has acquired the ability to survive and replicate by arresting phagosomal maturation. This phagosomal arrest has been correlated to the down-regulation of the Rab 10 gene and in order for the host cell to combat the infection the Rab10 gene must be up-regulated (Cardoso 2010). The up-regulation of Rab 10 allows the phagosome to fuse with a lysosome and to mature into a phagolysosome where the contents within the vesicle are degraded or recycled to the plasma membrane. This knowledge allows for inferences about how the competent *Symbiodinium* is infecting the coral gastrodermal cell.

Algal Maintenance

In this microarray analysis, Rab 10 is upregulated in the competent infection treatment, suggesting that at this time point, the polyp is decreasing the

numbers of zooxanthellae that have been allowed to replicate within its tissues. It is unclear as to whether the initial infection has caused a down-regulation in Rab10 as seen in the *Mycobacterium* infection. We would not necessarily expect to see down-regulation in *M. faveolata* at this time point being that a previous microarray (Voolstra *et al* 2009) has demonstrated that the competent symbiont has been taken up by day six. However, the polyp host could be reacting in the same manner as the parasitic host, as it strives to maintain a healthy internal environment after infection. Specificity by the host for the correct symbiont could be taking place at this time as the competent symbiont remains in the polyp but its numbers are reduced. The healthy maintainence of the symbiosis is perhaps now dependent upon regained endocytic recycling, so that the contents of the phagosome can be relayed to other organelles or the necessary receptors can return to the plasma membrane (Chen 2006).

A plausible explanation for the up-regulation of Rab 10 in *M. faveolata* at this time point is that the polyp is subjecting the *Symbiodinium* to a winnowing effect in order maintain a healthy symbiosis. This effect has been observed in the scyphistomae of the jellyfish *C. xamachana* when exposed to the different strains of the sybiont *S. microdriaticum*. The persistence of the symbiont was evaluated by following the fate of the phagocytosed algal cells in the scyphistomae and it was observed that despite algal cell division, the competent algal population in the scyphistomae declined within the following 2-3 days, stabilized over a period of 3-14 days, and then dramatically increased (Colley 1983). Our analysis looks at the ninth after day infection where symbiosome trafficking appears to be in

flux. This is perhaps done in order for the polyp to keep the zooxanthelle population below carrying capacity as it is known that *Symbiondinium* are continuously released from their hosts (Steele, 1977; Hoegh-Guldberg et al., 1987, Stimson and Kinzie, 1991) as the symbiont continues cell division and growth within the polyp.

Vesicular trafficking is clearly important in the process of phagocytosis, and also is important for synaptic transmission. The neurobeachin gene, found in mammalian CNS (Wang et al., 2000), that plays a general role in synaptic transmission and at the neuromuscular junction shares sequence similarity with a transcript (CAGI3054) that was up-regulated in this analysis. However, it is the evolutionary ancient C-terminal region of neurobeachin known as the BEACH domain that is most likely homologous between transcripts. Neurobeachin is thought to be involved in neuron-to-neuron transmission and may modulate non-neuronal vesicular trafficking and release as evidenced by the role of the BEACH proteins in the mouse and *Dictyostelium* (Su 2004). In our study, neurobeachin is further supporting evidence for the importance of vesicular trafficking in maintaining the symbiosis.

Additionally, the current 9 day post-infection microarray study of *M. faveolata* shows the up-regulation of the gene Arylsulfatase B, a glycosulfohydrolase involved with desulfation of sulfated polysaccharides. Arylsulfatase activity has been found in numerous genera of bacteria, and in the digestive glands of a variety of marine animals that consume algae (Hoshi and Moriya, 1980; Akagawa-Matsushita *et al*., 1992; Kim *et al*., 2005).. This enzyme

is thought to facilitate digestion and absorption of algal polysaccharides by cleaving the sulfate ester bonds in dietary polysaccharides The up-regulation of this gene suggests that maintenance of the symbiont population is very important in establishing the symbiosis.

This microarray captures the transient transcriptomic window where the symbiosis has already been established and is being maintained and now the codevelopment of the symbiont population and the polyp is observable through transcriptomic changes.

Development

Among the up-regulated competent specific genes in this study is the developmental gene Notch and its ligand, Jagged. Notch plays an important role in cell-to-cell communication and is enhanced in polyps that harbor the competent symbiont. A study in *Hydra* found that Notch promotes differentiation of nematoblasts and female germ cells (Käsbauer, 2006). It is known that Notch signaling has the potential to create two adjacent cells, which exclude each other (de Celis and Bray, 1997). This can be achieved by the repressed transcription of the Notch ligand in the Notch-responding cell and inhibition of the Notch-response in the signal-sending cell. This is demonstrated by another study in *Hydra* where it is found that Notch signaling is required in order for the formation of the critical boundary layer between the polyp and the asexual polyp bud to form and for the further differentiation of the bud's foot cells. The boundary is thought to be the result of a cascade effect where FGF-signaling is causing the

gene of one layer to produce the ligand, Jagged, which binds to the Notch receptor of the neighboring layer, and in turn activates the differentiation genes in the foot of the bud (Münder, 2010).

Infection with the competent symbiont Mf1.05b upregulates Notch transcription in *M. faveolata* and it can be inferred from studies in *Hydra* that this allows for successful sexual and asexual reproduction. Further, support for the positive affect of the competent symbiont upon the developing germline is the up-regulation of the gene Methionine aminopeptidase 2. In *C. elegans*, this gene is essential for germ cell development and when down-regulated, the gene contributes to sterility (Boxem, 2004). The genetic changes conferred upon the host by the symbiont could at this time be established within the germline as the symbiont itself up-regulates the sequestration of the germ cells and promotes cloning.

Calcification and Immune response

In support of the “light enhance calcification” theory, polyps that are infected with the competent symbiont show an up-regulation in one of the scleractinian cysteine-rich proteins. It was shown by Sunagawa et al., (2009) that this family of proteins groups into the same gene-expression cluster with galaxin, which was identified by Fukuda et al. (2003) as a major component of the calcifying organic matrix in the coral *Galaxia fascicularis* .The SCRiPs protein exhibits molecular features that suggests its involvement in biomineralization. First is the presence of a signal peptide region in order for localization to the extracellular matrix. Second, it is a cysteine-rich mature protein, which could

interact via disulfide-bonds with other cysteine-rich organic matrix molecules like galaxin (Sunagawa et al., 2009).

While the transcript for this cysteine-rich protein is up-regulated, the proteins that are capable of reducing the SCRiPs protein are also up-regulated. This includes gamma-interferon-inducible lysosomal thiol reductase and thioredoxin. However, it has been found that a rise in intracellular calcium induced by growth factors binding to their receptors results in the conversion of reduced thioredoxin to its oxidized form (Gitler, 2002). This results in the inhibition of thiorexodin reductase coupled to a rise in the formation of peroxide and subsequent redox changes which affects thiols and facilitate mitogen signal transduction. What this suggests for the polyp is that calcium sequestration may continue because the cell is maintaining equilibrium through the use of calcium during growth. Additionally, the calcium binding complex calbindin-32 is also shown to be up-regulated in this analysis. Calbindin acts as a calcium buffer and as a sensor that allows for calcium to cross cell membranes without raising its free concentration (Reifegerste, 1993).

Classic immune response genes such as the superoxide dismutases (SODs) are up-regulated in the competent infection transcriptome. This class of enzymes catalyzes the dismutation of superoxide into oxygen and hydrogen peroxide. As such, they are an important antioxidant defense in nearly all cells exposed to oxygen. Additionally, peroxidasin is up-regulated and it serves to oxidize organic substrates in the presence of hydrogen peroxide. The CCAAT/enhancer-binding protein gamma known to enhance immune and

inflammatory responses is also up-regulated (Akira et al., 1990), further regulating the immune response.

In the competent infection, apoptosis is occurring as evidenced by the presence of a E3 ubiquitin-protein ligase LRSAM1 homolog up-regulation. In conjunction with the E2 ubiquitin-conjugating enzyme, ubiquitin is attached to a lysine on the targeted protein and the polyubiquination signals for degradation by the proteosome. Apoptosis is important for healthy development in any organism and also plays a role here.

Incompetent infection

Of the polyp samples exposed to the incompetent algae strain EL1, significant gene down-regulation is seen. The genes primarily affected are genes responsible for eukaryotic ribosomal proteins, such as 60S ribosomal protein L10, L18a, L13, L7a, L13, P0, P1, and 40S ribosomal protein S12, S11, S10. Ribosomal proteins are necessary for the ribosomal subunits to function; this suggests that translation is being negatively affected.

Additionally, the 10kDa heat shock protein of the mitochondria is down-regulated, suggesting less chaperone activity to correct for protein folding problems. The mitochondrial import receptor subunit TOM40 is downregulated. This is the translocase of the outer mitochondrial membrane and it is the means by which proteins enter into the mitochondria. Cytochrome c transcription is down-regulated as well. Cytochrome c is essential in the electron transport chain of the mitochondria, therefore it can be assumed that the energetic requirements

of the developing polyp's cells are not being met when infected with the incompetent algae EL1.

Furthermore, tubulin is down-regulated in this treatment and may be causing a cease in very important vesicle trafficking. Ubiquitin is down-regulated, suggesting that apoptosis is not fully operative and no longer managing healthy development. The cells also react to the incompetent infection with the up-regulation of histone deacetylases, which promote chromatin remodeling and cause heterochromatin formation, resulting in chromosome compaction and altered gene transcription.

The results of this study when compared to previous experimentation on *Acropora millepora* polyp settlement show novel genes that are differentially expressed that may be a direct result of the effect the competent symbiosis has on the calcifying polyp, aside from the genes known to be involved in the process of settlement in an uninfected polyp. The genes that showed significant differential expression in the settlement induction experiment included genes concerning calcium handling, apoptosis, immunity, stress response, calcium metabolism, formation of the skeletal organic matrix, calcium-sequestering proteins (calreticulin), protein folding (heat shock proteins), cell adhesion (lectins). We additionally found developmental genes and vesicular genes to be significantly differentially expressed with the symbioses is established and maintained. At an earlier time point, during the establishment of the coral-algal symbiosis, it was observed that the host transcriptome remains unaltered by infection with the competent symbiont. In this study we see a more significant

change in the transcriptome of the polyp exposed the competent infection suggesting that the competent symbiont is now a noticed and exchangeable entity with in the coral tissue.

The above microarray results have been qualified by qPCR (Figure 4). However, microarray results do not substitute for functional studies. The next step would be to employ molecular techniques such as RNA interference, morpholino injection and/or in situ hybridization in order to better understand the roles of the genes required for the codevelopment of *Montastraea faveolata* and *Symbiodinium.* The knockdown of lectins on the polyp's cell surface and/or the knockdown of the Rab10 protein point in the direction of resolving just how the host recognizes the competent symbiont in the coral/algal symbiosis. The other side of this study would be to look at the affect the host has on the development of the symbiont. It can be assumed that at a point in development, the algae's cell division is controlled by the host perhaps in a density dependent manner, until such a study is preformed this remains speculation.

It is through large transcriptomic studies like this one, and its comparison to others, that we are able to identify the genes that are shared throughout the unicellular and multicellular world. This allows us to gain a better knowledge of how species interact and how they differ with other species both environmentally and genetically. It is important for the future of coral reefs to keep in mind that the gradual process of evolution has brought different organisms together, such as the coral and its symbionts. It is of scientific interest and social interest to

understand these mutualisms and to conserve this ecosystem, as it is an ancient foothold in the web of life.

References

Smith, S.E. and. D.J. Read. (1997) Mycorrhizal Symbiosis (2nd Edition). 605 pp. Academic Press, San Diego and London.

Bates, S.T., Cropsey, G.W., Caporaso, J.G., Knight, R. et al., (2011) Bacterial communities associated with the lichen symbiosis. Appl. Environ Microbiol.

Grasso LC, Negri AP, Foret S, Saint R, Hayward DC and Ball EE (2011) The biology of coral metamorphosis: Molecular responses of larvae to inducers of settlement and metamorphosis. Developmental Biology 353: 411-419

Nyholm, S. V. & McFall-Ngai, M. J. (2004) The winnowing: establishing the squid-vibrio symbiosis. Nat. Rev. Microbiol. 2, 632–642.

Dedeine, F., Vavre, F., Fleury, F., Loppin, B., Hochberg, M. E. & Bouletreau, M. (2001) Removing symbiotic Wolbachia bacteria specifically inhibits oogenesis in a parasitic wasp. Proc. Natl Acad. Sci. USA 98, 6247–6252.

Nguyen L, Pieters J (2005) The Trojan horse: Survival tactics of pathogenic mycobacteria in macrophages. *Trends Cell Biol*ogy. 15(5): 269-276.

Schwarz, J.A. (2008). Understanding the intracellular niche in cnidarian-*Symbiodinium* symbioses: parasites lead the way. Vie et Millieu: Life and the Environment. 58 (2): 141-151.

Clode PL, Marshall AT. (2004) Calcium localisation by X-ray microanalysis and fluorescence microscopy in larvae of zooxanthellate and azooxanthellate corals. Tissue Cell;36:379–90

Reyes-Bermudez A, DeSalvo MK, Voolstra CR, Sunagawa S, Szmant AM, Iglesias-Prieto R, Medina M (2009). Gene expression microarray analysis encompassing metamorphosis and the onset of calcification in the scleractinian coral Montastraea faveolata. Mar Genomics.

Kawaguti, S., and D. Sakumoto (1948). The effect of light on the calcium deposition of corals. *Bull. Oceanogr. Inst. Taiwan* 4:65–70.

Hinde, R and D. Trautman (2004) Symbiosomes. Cellular Origin, Life in Extreme Habitats and Astrobiology, Volume 4, II, 207-220, DOI: 10.1007/0-306-48173-1_12

Fitt WK, Trench RK (1983) Endocytosis of the symbiotic dinoflagellate *Symbiodinium microadriaticum* Freudenthal byendodermal cells of the scyphistomae of *Cassiopeia xamachana* and resistance of the algae to host digestion. *J Cell Sci* 64: 195-212.

Schwarz, J.A., D.A. Krupp, and V.M. Weis (1999) Late larval development and onset of symbiosis in the scleractinian coral Fungia scutaria. Biological Bulletin 196: 70-79

Schnitzler, C. E. and V. M. Weis (2010) Coral larvae exhibit few measurable transcriptional changes during the onset of coral-dinoflagellate endosymbiosis. *Marine Gemomics* 3:107-116

Voolstra, C.R., J.A. Schwarz, J. Schnetzer, S. Sunagawa, M.K. DeSalvo, A.M. Szmant, M.A. Coffroth, M. Medina (2009). The host transcriptome remains unaltered during the establishment of coral-algal symbioses. Mol Ecol: 18(9), 1823-1833.

Frazier, W., and Glaser, L. (1979) Surface components and cell recognition. Annu. Rev. Biochem. 48:491-523.

Muscatine L. & Pool, R. (1979). Regulation of numbers of intracellular algae. *Proc. R. Soc. Lond.* B, 204, 131-139.

E.M. Wood-Charlson, V.M. Weis /Developmental and Comparative Immunology 33 (2009) 881–889.

Cardoso C. M., M. L. Jordao and O. V. Vieira* (2010). Rab10 is required for phagosome maturation and its overexpression can change the fate of Mycobacterium-containing phagosomes. *Traffic*, 11(2):221-35.

Steele, R. D. (1977) The significance of zooxanthellae-containing pellets extruded by sea anemones. *Bull. Mar. Sci.* 27: 591–594.

Stimson, J., and R. A. Kinzie (1991) The temporal pattern and rate of release of zooxanthellae from the reef coral *Pocillopora damicornis* (Linnaeus) under nitrogen-enrichment and control conditions. *J. Exp. Mar. Biol. Ecol.* 153: 63–74.

Hoegh-Guldberg, O., L. R. McCloskey, and L. Muscatine. (1987) Expulsion of zooxanthellae by symbiotic cnidarians from the Red Sea. *Coral Reefs* 5: 201–204.

Chen, C. C., P. J. Schweinsberg, S. Vashist, D. P. Mareiniss, E. J. Lambie *et al.*, (2006) RAB-10 is required for endocytic recycling in the *Caenorhabditis elegans* intestine. *Mol. Biol. Cell* 17 1286–1297

Wang X, Herberg FW, Laue MM, Wullner C, Hu B, Petrasch-Parwez E, Kilimann MW (2000) Neurobeachin: a protein kinase A-anchoring, beige/Chediak-higashi protein homolog implicated in neuronal membrane traffic. J Neurosci 20: 8551–8565.

Su (2004) Neurobeachin Is Essential for Neuromuscular Synaptic Transmission

Hoshi, M., and Moriya, T. (1980) Arylsulfatase of sea-urchinsperm. 2. Arylsulfatase as a lysine of sea-urchins. *Dev Biol*74: 343–350.

Akagawa-Matsushita, M., Matsuop, M., Koga, Y., and Yamasato, K. (1992) *Alteromonas atlantica* sp. nov. and *Alteromonas carrageenovora* sp. nov. bacteria that decompose algal polysaccharides. *Int J Syst Bacteriol* 42: 621–627.

Kim, D.-E., Kim, K.-H., Bae, Y.-J., Lee, J.-H., Jang, Y.-H., and Nam, S.-W. (2005) Purification and characterization of the recombinant arylsulfatase cloned from *Pseudoalteromonas carrageenovora*. *Protein Expr Purif* 39: 109–115.

Käsbauer, T., Towb, P., Alexandrova, O., David, C.N., Dall'armi, E., Staudigl, A., Stiening, B., Böttger, A. (2006). The Notch signaling pathway in the cnidarian Hydra. Dev. Biol. 303 (1), 376–390.

de Celis, J.F., Bray, S. (1997). Feed-back mechanisms affecting Notch activation at the dorsoventral boundary in the Drosophila wing. Development 124(17): 3241--3251.

Munder S., KaÅNsbauer T., Prexl A., Aufschnaiter R, Zhang X., Towb P., BoÅNttger A. (2010) Notch signaling defines critical boundary during budding in *Hydra* // *Dev. Biol*. 344(1): 331-45.

Gajewski, M., Leitz, T., Schlossherr, J. and Plickert, G. (1996) Lwamides from Cnidaria constitute a novel family of neuropeptides with morphogenetic activity. *Rouxs Arch. Dev. Biol.* 205, 232–242.

Boxem M, Tsai CW, Zhang Y, Saito RM, Liu JO (2004) The C. elegans methionine aminopeptidase 2 analog map-2 is required for germ cell proliferation. FEBS Lett 576: 245–250

Greer EL and Brunet A. FOXO transcription factors at the interface between longevity and tumor suppression. (2005) Oncogene, 24: 7410-7425.

Fukuda I, Ooki S, Fujita T, Murayama E, Nagasawa H, et al. (2003) Molecular cloning of a cDNA encoding a soluble protein in the coral exoskeleton. Biochem Biophys Res Commun 304: 11–17.

Sunagawa, S., M.K. DeSalvo, C.R. Voolstra, A. Reyes-Bermudez, M. Medina (2009). Identification and Gene Expression Analysis of a Taxonomically Restricted Cysteine-Rich Protein Family in Reef-Building Corals. PLoS ONE 4(3): 4(3).

Gitler C., Zarmi B., Kalef E., Meller R., Zor U., Goldman R . (2002) Calcium-dependent oxidation of thioredoxin during cellular growth initiation. *Biochem. Biophys. Res. Commun*; 290:624–628.

Reifergerste R, Grimm S, Albert S, et al. (1993) An invertebrate calcium-binding protein of the calbindin subfamily: protein structure, genomic organization and expression pattern of the calbindin-32 gene of *Drosophila*. *J Neuroscience*.;13:2186-2198.

Akira, S., Isshiki, H., Sugita, T., Tanabe, O., Kinoshita, S., Nishio, Y., Nakajima, T., Hirano,T., Kishimoto, T. (1990) A nuclear factor for IL-6 expression (NF-IL6) is a member of a C/EBP family. EMBO J. 9, 1897–1906.